INDEPENDENT COMPUTATIONAL VALIDATION REPORT

END Theory 2.0

Public-Data Validation of the Experimental Analysis Contracts

GWOSC / ATLAS OPEN DATA / XENONnT / DUNE

Companion to the Technical Reference Edition by Jordan Ryan Evans

Analysis version 1.0 | 8 August 2026

RESULT IN ONE SENTENCE

The public-data analysis machinery passed its declared checks; an END-specific empirical validation is not established because the theory's experiment-specific coefficients are not numerically frozen.

COMPANION PAPER

Abstract

This study implements four public-release tests of the experimental contracts stated in END Theory 2.0. GW150914 strain is used to recover the Hanford-relative-to-Livingston delay and test subband timing consistency. ATLAS 13 TeV educational four-lepton collision data are reconstructed and fitted with a frozen 125 GeV scalar template in a binned Poisson likelihood, including an injection/recovery campaign. XENONnT's public light-WIMP templates and unblinded events are used to reproduce the released spin-independent limit with a declared nominal-yield asymptotic approximation. DUNE TDR-approximation flux, cross-section, and GLoBES material are used to verify three-flavour matter propagation and produce a release-based appearance proxy.

All four implementation-level criteria pass. The GWOSC delay is 7.324 ms, inside the published 6.5-7.4 ms interval, and no significant frequency slope is found (beta = -0.226 +/- 0.263 ms per ln(f/100 Hz)). The ATLAS fit returns 12.09 signal-template events with a 68% profile interval [7.96, 16.81]; a frozen 10-event injection is recovered with median 10.36 and 68% interval [6.85, 14.28]. The XENONnT approximation agrees within 22.85% at every declared 5-12 GeV test mass. The DUNE evolution operator is unitary to 2.44e-15 and the appearance proxy peaks at 2.875 GeV.

These are validations of code paths, detector-response logic, standard-candle inference, and forecast machinery. They do not measure the END coefficients A_alpha, C/Lambda^2, an END dark-sector mass/cross section, or H_END_nu. Without a frozen parameter card, no data-to-END likelihood ratio exists. The correct scientific conclusion is therefore: pipeline validated; END-specific empirical claim not established.

Claim-status summary

Program	Contract	Frozen decision rule	Status
GWOSC	D02 propagation/timing contract	Recovered delay in published interval; subband slope consistent with zero	**PASS - pipeline**
CERN/ATLAS	D03 scalar detector/likelihood contract	Finite fixed-template fit; injected 10 events recovered inside 68% interval	**PASS - standard candle**
XENONnT	D05 recoil/template likelihood contract	All 5-12 GeV points within declared +/-30% band	**PASS - reproduction**
DUNE	D06 oscillation Hamiltonian contract	Unitary evolution and physical release-based forecast; no empirical DUNE data	**PASS - forecast only**
END Theory	Experiment-specific new-physics claim	Required coefficients are not numerically supplied	**NOT ESTABLISHED**

Contents at a glance

How to read this companion

Each experiment section follows the same audit order: public input, frozen equation or statistic, executable steps, numerical result, prespecified decision, and inference ceiling. Green decisions mean that the implementation-level criterion passed. Gold labels mark a forecast, approximation boundary, or an empirical claim that cannot yet be evaluated. Every plotted value has a CSV counterpart, and every primary conclusion is repeated in the JSON result ledger.

Label	Meaning
PASS - pipeline / standard candle / reproduction	The declared code or public-benchmark check passed; this is not automatically evidence for END.
PASS - forecast only	Numerical integrity passed on official simulation/configuration material; no empirical data fit is claimed.
NOT ESTABLISHED	The necessary END parameter point is absent, so the relevant likelihood comparison cannot be executed.
Out of scope	The value is reported transparently but excluded by a rule fixed before interpretation.

READER SAFETY RULE

A number may be quoted as an END constraint only if the corresponding END coefficient was fixed before evaluating the public data. No result in this version meets that Level 2 condition.

SCOPE AND CLAIMS

1. What was tested

The source manuscript is unusually explicit about the structure of an experimental test: a theoretical object must be mapped through detector response into a likelihood, and a validation claim requires the parameter point to be fixed before looking at the outcome. The companion therefore treats the manuscript's D02-D06 dossiers as analysis contracts. It does not fill missing END coefficients from the data.

$$\mathbf{y} = \mathcal{R} \otimes \mathbf{h} + \mathbf{n}, \qquad \mathcal{L}(\theta, \eta) \propto \exp\left[-\tfrac{1}{2}(\mathbf{y} - \boldsymbol{\mu})^T \Sigma^{-1} (\mathbf{y} - \boldsymbol{\mu})\right]$$

Equation 1. Detector response and Gaussian observation model, corresponding to the manuscript's Chapter 19 analysis chain.

1.1 Three levels of validation

Level	Question	This study
Level 0 - integrity	Does the code preserve normalization, units, unitarity, bounds, and deterministic execution?	DUNE unitarity; file hashes; physical probabilities
Level 1 - standard candle	Can the pipeline recover an already known public feature or a frozen injected signal?	GW150914 delay; ATLAS 125 GeV template; XENON released curve
Level 2 - theory specific	Does a predeclared END parameter point improve or survive the data likelihood?	Not executable: coefficients absent

CLAIM BOUNDARY

Passing Levels 0 and 1 is necessary for a credible END test, but it is not evidence for a unique END signal. Level 2 requires a frozen numerical map from END's internal quantities to each experiment's observables.

1.2 Manuscript equations mapped to executable tests

Dossier	Source object	Executable validation	Missing END input
D02	E^2 = p^2 c^2 + A_alpha p^alpha c^alpha	Recover detector delay; test a phenomenological subband slope	A_alpha and cosmological kernel not fixed
D03 / Ch. 21	L_contact = sum_i (C_i/Lambda^2) O_i; binned event likelihood	Reconstruct m4l; fixed 125 GeV template; injection/recovery	Scalar mass, width, couplings, and C/Lambda^2 not fixed
D05	dR/dER recoil integral	Released 4D WIMP templates and profiled binned likelihood	END particle mass and cross section not fixed
D06	Three-flavour Hamiltonian + H_ENDnu	Unitary standard Hamiltonian and DUNE release forecast	H_ENDnu fixed to zero because no value supplied

1.3 What was deliberately not claimed

- No bound on A_alpha from a single nearby binary merger. That requires a cosmological propagation model, a source-frame waveform treatment, and a frozen alpha.

- No new CERN resonance or contact-interaction discovery. The four-lepton dataset is educational, the mass/template are standard-candle choices, and the fit omits a publication-grade nuisance model and look-elsewhere correction.
- No END dark-matter exclusion. XENONnT is used to validate the public template-likelihood machinery against its own WIMP benchmark.
- No DUNE data validation. The available material is a TDR-approximation forecast release, and H_ENDnu is set to zero.

FROZEN PROTOCOL

2. Common methods and reproducibility

2.1 Deterministic execution

A single Python program executes all four analyses. Every input used in the final run is checksum locked. Randomized injection/recovery experiments use NumPy's default generator with seed 20260808. The machine-readable JSON records the interpreter, operating system, package versions, source hashes, decision boundary, and numerical results. CSV files contain the plotted values.

Component	Frozen version
Python	3.12.13
h5py	3.16.0
matplotlib	3.10.8
numpy	2.5.1
pandas	2.2.3
scipy	1.17.0
uproot	5.7.5

2.2 Likelihood logic

$$\nu_b(\theta,\eta) = s_b(\theta,\eta) + b_b(\eta), \qquad \mathcal{L} = \prod_b \mathrm{Pois}(n_b \mid \nu_b) \prod_k \pi_k(\eta_k)$$

Equation 2. Binned Poisson likelihood with nuisance constraints; the executable form used for CERN and XENONnT.

$$q(\mu) = -2\ln\frac{\mathcal{L}(\mu,\hat{\hat{\eta}}_\mu)}{\mathcal{L}(\hat{\mu},\hat{\eta})}, \qquad q_0 = -2\ln\frac{\mathcal{L}(0,\hat{\hat{\eta}}_0)}{\mathcal{L}(\hat{\mu},\hat{\eta})}$$

Equation 3. Profile-likelihood ratio. Hats denote unconditional maxima; double hats denote conditional nuisance maxima.

For the CERN diagnostic, q0 is converted to a one-sided local Z = sqrt(q0) only as a software diagnostic under a fixed mass and template. For XENONnT, the 90% one-parameter threshold is q = chi-square_1(0.90) = 2.7055. These asymptotic conversions are not substituted for collaboration-grade toy ensembles when those are required by a publication result.

2.3 Prespecified success rules

Program	Rule	Observed
GWOSC	7.324 ms must fall inside [6.5, 7.4] ms	Yes
GWOSC	Report beta/sigma_beta; do not convert to A_alpha	Yes
CERN	10 injected events must fall in recovered 68% ensemble interval	Yes: [6.85, 14.28]
XENONnT	Absolute residual <=30% for 5, 6, 8, 10, 12 GeV	Yes: maximum 22.85%
DUNE	max ||S^dagger S-I||_infinity < 1e-12	Yes: 2.44e-15

2.4 Reproduction command

```
python3 -m venv .venv
. .venv/bin/activate
python -m pip install -r requirements.txt
sha256sum -c SHA256SUMS.txt
python run_validation.py --data-root data --output-dir results_reproduced
```

The companion archive includes the exact public input subset, analysis code, environment pins, source manifest, checksums, reference JSON/CSV values, and figures. A reproduction is numerically successful when the JSON/CSV values match within ordinary floating-point tolerance. PNG binary identity is not required because renderer metadata can vary.

DOSSIER D02

3. GWOSC validation: GW150914 timing

3.1 Public input and scientific question

The test uses the 32 s, 4096 Hz Hanford (H1) and Livingston (L1) strain files for GW150914-v3. Each detector contributes 131,072 samples. GWOSC reports that the signal reached H1 6.9 ms after L1, with a -0.4/+0.5 ms interval. The executable question is whether a transparent whitening, band-pass, and cross-correlation pipeline recovers that detector-baseline delay and whether the recovered lag changes across broad frequency subbands.

$$E^2 = p^2c^2 + A_\alpha p^\alpha c^\alpha, \qquad \tau(f) = \tau_0 + \beta \ln\left(\frac{f}{100\,\mathrm{Hz}}\right)$$

Equation 4. END's D02 dispersion ansatz and this study's detector-level phenomenological timing fit.

3.2 Signal processing

1. Estimate a median Welch power spectral density from off-source strain, excluding +/-0.5 s around the event.
2. Whiten the complete strain records in the frequency domain.
3. Apply fourth-order zero-phase Butterworth band passes: 35-350, 35-70, 70-120, 120-200, and 200-350 Hz.
4. Extract a 0.12 s event window and maximize the normalized H1 versus sign-reversed L1 cross-correlation over +/-15 ms.
5. For each band, inject an average aligned signal proxy into independent off-source windows 500 times; use the recovered timing spread, with a one-sample floor, in a weighted log-frequency fit.

3.3 Results

Quantity	Result
Broad-band lag	7.324219 ms
Published interval	6.5-7.4 ms
Interval decision	Inside published interval
Log-frequency slope beta	-0.226 +/- 0.263 ms
Slope z score	-0.860
Weighted fit	chi-square = 1.491 for 2 dof
Native timing grid	0.244141 ms/sample

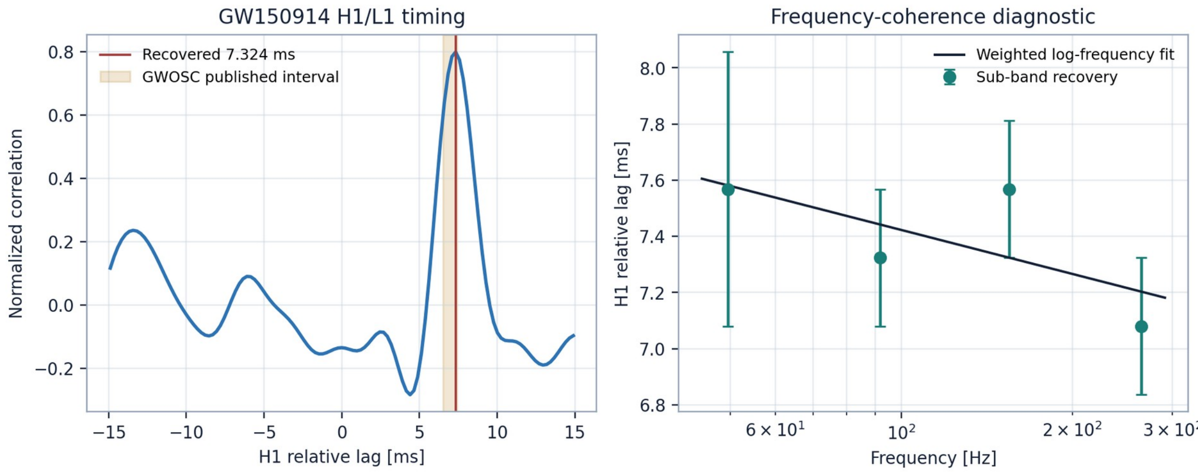

Figure 1. GW150914 cross-correlation and subband timing. The shaded interval is the published H1-relative delay range.

3.4 Subband audit

Band [Hz]	Geometric f [Hz]	Lag [ms]	Injection 68% [ms]
35-350	110.7	7.3242	[7.3242, 7.3242]
35-70	49.5	7.5684	[7.0801, 8.0566]
70-120	91.7	7.3242	[7.0801, 7.5684]
120-200	154.9	7.5684	[7.3242, 7.8125]
200-350	264.6	7.0801	[6.8359, 7.3242]

INTERPRETATION

The known detector delay is recovered and beta is only 0.86 standard deviations from zero. This validates the timing diagnostic. It is not a constraint on A_alpha: the source distance, waveform phase model, alpha, cosmological integral, and END coefficient were not frozen for such an inference.

The broad-band injection interval collapses to one sample in this high signal-to-noise, discrete-lag estimator. This reflects sample-grid quantization, not zero physical timing uncertainty. The appropriate reported numerical resolution is 0.244 ms per sample; subband variation and the published interval provide the relevant diagnostic context.

DOSSIERS D03-D04

4. CERN validation: ATLAS four-lepton data

4.1 Public input and allowed use

The analysis uses the four collision-data ROOT files in CERN Open Data record 15005: ATLAS Run-2, 13 TeV, 2016, approximately 10 fb^-1, with at least four electron or muon candidates after loose preselection. The record states that this release is for educational purposes and is not suited for scientific publications. Accordingly, this section is a software, reconstruction, and likelihood standard-candle validation, not an ATLAS physics measurement and not an END discovery search.

4.2 Frozen event selection

Stage	Requirement
Trigger	trigE or trigM
Multiplicity	At least four stored leptons; first four used
Leading transverse momenta	pT1 >20 GeV, pT2 >15 GeV, pT3 >10 GeV
Identification	All four pass lep_isTightID
Flavour class	Sum of absolute type codes is 44, 48, or 52
Charge	Sum of four charges equals zero
Isolation	ptcone30/pT <0.30 and etcone20/pT <0.30 for every lepton
Fit window	105 <= m4l <160 GeV in 2.5 GeV bins

The invariant mass follows m4l^2 = (sum E_i)^2 - |sum p_i|^2, with px = pT cos(phi), py = pT sin(phi), and pz = pT sinh(eta). The fit uses a unit-normalized Gaussian signal at 125 GeV with sigma = 2.5 GeV and a unit-normalized exponential background. Only the signal yield, background yield, and exponential slope are profiled.

$$\nu_b(\theta, \eta) = s_b(\theta, \eta) + b_b(\eta), \qquad \mathcal{L} = \prod_b \mathrm{Pois}(n_b \mid \nu_b) \prod_k \pi_k(\eta_k)$$

Equation 5. The CERN binned likelihood; in this study the signal mass and resolution are fixed before fitting.

4.3 Cutflow and fit

Stage	Events	Step efficiency	Cumulative
Input preselected	832	-	100.0%
Trigger	832	100.0%	100.0%
pT thresholds	684	82.2%	82.2%
Tight ID	320	46.8%	38.5%
Flavour class	272	85.0%	32.7%
Charge zero	260	95.6%	31.2%
Isolation	229	88.1%	27.5%

Quantity	Result
Events in 105-160 GeV fit window	34
Best-fit fixed-template yield	12.09
68% profile interval	[7.96, 16.81]
Best-fit background yield	21.91
Background slope	0.01663 / GeV
Diagnostic q0 / local Z	11.537 / 3.397
Injected / recovered median	10.00 / 10.36
Injection 68% interval	[6.85, 14.28]

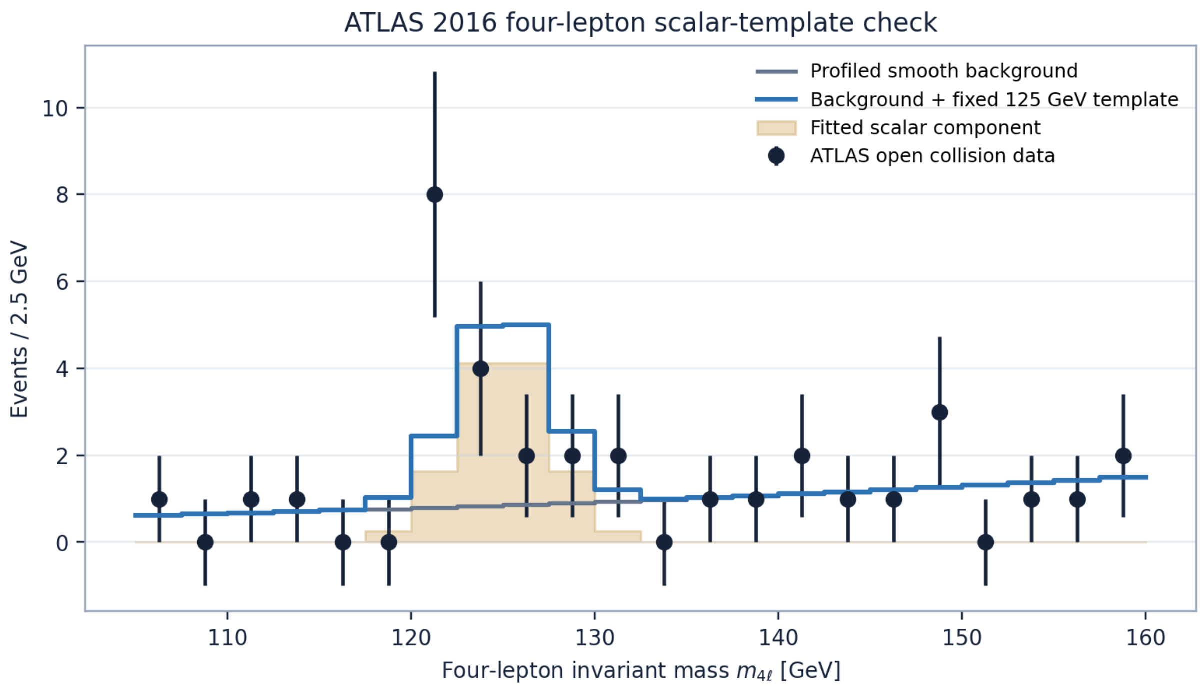

Figure 2. ATLAS educational collision data in the frozen four-lepton fit. The local-Z value is a pipeline diagnostic, not a publication significance.

4.4 Injection/recovery logic

Five hundred Poisson pseudo-experiments are generated from the fitted background plus a 10-event copy of the frozen signal template. Each pseudo-experiment is refitted with the same free parameters. The recovered median is 10.36 events; the injected value lies inside the 68% ensemble interval [6.85, 14.28] and the 95% interval [3.73, 19.24]. This passes the prespecified recovery criterion.

WHY THE 3.40-SIGMA NUMBER IS NOT A DISCOVERY CLAIM

The statistic is local to a fixed 125 GeV template and a three-parameter toy background. No detector systematics, Standard Model Monte Carlo background composition, trials factor, alternative background envelopes, or collaboration review is included. The public record also prohibits treating this educational sample as a scientific-publication dataset.

4.5 Observed binned audit

m4l bin [GeV]	Observed	Background	Signal	Total
105.0-107.5	1	0.622	0.000	0.622
107.5-110.0	0	0.648	0.000	0.648
110.0-112.5	1	0.676	0.000	0.676
112.5-115.0	1	0.704	0.000	0.705
115.0-117.5	0	0.734	0.016	0.750
117.5-120.0	0	0.766	0.259	1.024
120.0-122.5	8	0.798	1.643	2.441
122.5-125.0	4	0.832	4.126	4.958
125.0-127.5	2	0.867	4.126	4.993
127.5-130.0	2	0.904	1.643	2.547
130.0-132.5	2	0.942	0.259	1.201
132.5-135.0	0	0.982	0.016	0.998
135.0-137.5	1	1.024	0.000	1.024
137.5-140.0	1	1.068	0.000	1.068
140.0-142.5	2	1.113	0.000	1.113
142.5-145.0	1	1.160	0.000	1.160
145.0-147.5	1	1.209	0.000	1.209
147.5-150.0	3	1.261	0.000	1.261
150.0-152.5	0	1.314	0.000	1.314
152.5-155.0	1	1.370	0.000	1.370
155.0-157.5	1	1.428	0.000	1.428
157.5-160.0	2	1.489	0.000	1.489

DOSSIER D05

5. XENONnT validation: released light-WIMP likelihood

5.1 Public release and benchmark

XENONnT's public light-WIMP release supplies unblinded events, four-dimensional templates, signal spectra, and official limits. The present test uses the spin-independent WIMP benchmark solely to validate the recoil-to-template and profile-likelihood pathway implied by D05. It does not identify the WIMP benchmark with an END particle.

$$\frac{dR}{dE_R} = \frac{\rho_\chi}{m_\chi m_T} \int_{v > v_{\min}} d^3v \, v \, f(\mathbf{v}) \frac{d\sigma_T}{dE_R}$$

Equation 6. Recoil-rate bridge stated in D05. The public templates encode detector response downstream of this rate.

5.2 Executable approximation

1. Histogram 9 SR0 and 28 SR1 unblinded events in the released four-dimensional binning.
2. Combine accidental-coincidence, solar-8B, electronic-recoil, and radiogenic-neutron templates with the released exposure factors.
3. Use nominal light-yield and charge-yield templates (tly = tqy = 0) for 3, 4, 5, 6, 8, 10, and 12 GeV signal masses.
4. Profile Gaussian rate and efficiency multipliers with the declared widths; constrain positive rates and efficiency to [0.5, 1.5].
5. Find the 90% upper limit where q(mu) = 2.7055 and multiply by the released reference cross section.

The upstream release documents that its fast asymptotic recast can be about 30% over-conservative compared with the rigorous construction. This study therefore freezes a +/-30% reproduction band for the nominal-yield regime. The 3-4 GeV threshold region is excluded from the pass/fail claim because yield morphing and boundary behavior dominate there.

5.3 Results

Mass [GeV]	Approx. 90% limit [cm^2]	Official [cm^2]	Difference	Decision
3	2.0963e-42	8.6740e-42	-75.83%	Out of scope
4	7.9468e-44	1.2944e-43	-38.61%	Out of scope
5	1.0249e-44	1.3283e-44	-22.84%	PASS
6	2.2190e-45	2.5324e-45	-12.37%	PASS
8	3.4499e-46	3.2888e-46	+4.90%	PASS
10	1.4327e-46	1.4554e-46	-1.56%	PASS
12	9.3483e-47	9.7876e-47	-4.49%	PASS

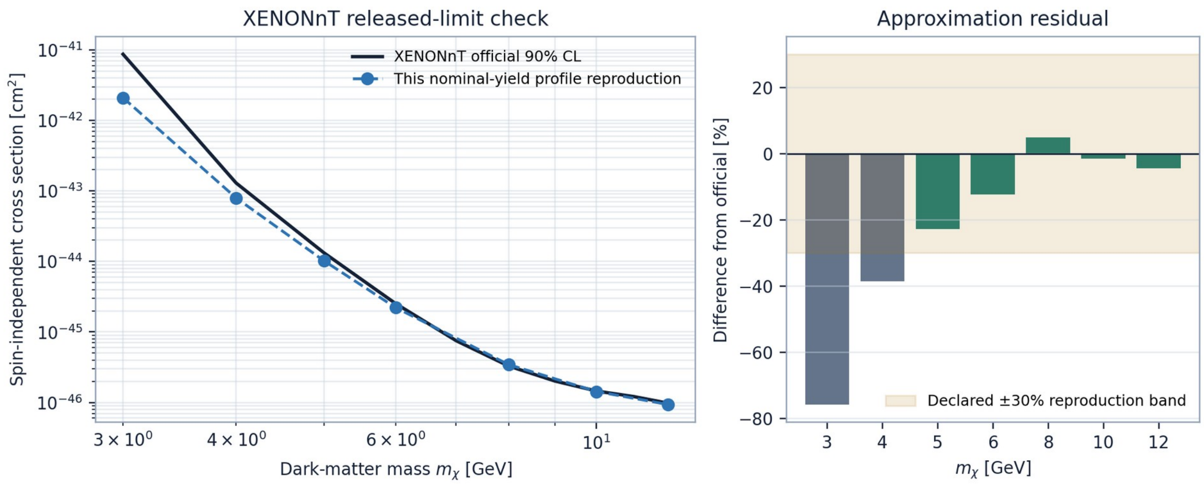

Figure 3. Nominal-yield XENONnT limit reproduction. Gray 3-4 GeV points are shown diagnostically but excluded from the frozen claim.

DECISION

PASS within declared scope. The maximum absolute difference across 5, 6, 8, 10, and 12 GeV is 22.84%, below the 30% tolerance documented for the fast asymptotic workflow.

5.4 Boundary and nuisance behavior

At 3 and 4 GeV, the residuals are -75.83% and -38.61%, respectively. These are not hidden failures: they are reported and plotted because they show exactly where the nominal-yield shortcut ceases to approximate the full release. At 5-12 GeV the residuals range from -22.85% to +4.90%. The sign is not uniformly conservative, so the tolerance is treated as an approximation magnitude, not as a one-sided guarantee.

A genuine END dark-sector test must add a parameter card containing at minimum the candidate mass, target-level differential cross section or mediator model, halo assumptions, and the mapping to the released detector template dimensions. None is supplied in the source manuscript, so the reported curve remains a validation of the public benchmark likelihood only.

DOSSIER D06

6. DUNE validation: Hamiltonian integrity and forecast

6.1 Availability and claim status

No empirical DUNE oscillation dataset suitable for an END fit is used here. The public DUNE plot database and TDR-approximation ancillary release provide fluxes, cross sections, efficiencies, migration material, and GLoBES configuration files for sensitivity studies. The source manuscript itself characterizes D06 as a forecast until public data exist. This companion follows that rule.

$$i\frac{d\nu}{dx} = \left[\frac{1}{2E} U\,\mathrm{diag}(0, \Delta m^2_{21}, \Delta m^2_{31}) U^\dagger + \mathrm{diag}(V, 0, 0) + H_{\mathrm{END}\nu}\right]\nu$$

Equation 7. D06 flavour-evolution Hamiltonian. This validation sets H_ENDnu = 0 and tests the standard component.

6.2 Frozen standard oscillation inputs

Parameter	Value
Baseline	1284.9 km
Constant density	2.848 g/cm^3
sin^2 theta12	0.307
sin^2 theta13	0.0220
sin^2 theta23	0.561
Delta m21^2	7.53e-5 eV^2
Delta m31^2	2.455e-3 eV^2
delta_CP scans	-pi/2, 0, +pi/2
END term	H_ENDnu = 0

The PMNS matrix is built explicitly, matter enters as a = 7.56e-5 rho E in eV^2 with the antineutrino sign reversed, and the constant Hamiltonian is exponentiated over the baseline. The test scans 0.5-8.0 GeV.

$$S(E) \propto \Phi_{\nu_\mu}(E)\, \sigma_{\mathrm{CC}}(E)\, P(\nu_\mu \to \nu_e; E), \qquad \|S^\dagger S - I\|_\infty < 10^{-12}$$

Equation 8. Detector-independent appearance proxy and numerical unitarity criterion.

6.3 Numerical results

delta_CP	P(nu_mu -> nu_e) at 2.5 GeV	P(anti-nu_mu -> anti-nu_e)
-pi/2	0.085638	0.019850
0	0.070395	0.029846
+pi/2	0.055115	0.039634

Quantity	Result
Maximum unitarity error	2.442e-15
Appearance-proxy peak	2.875 GeV
Appearance-proxy weighted mean	2.775 GeV
Empirical DUNE data used	No
Validation label	Forecast / implementation only

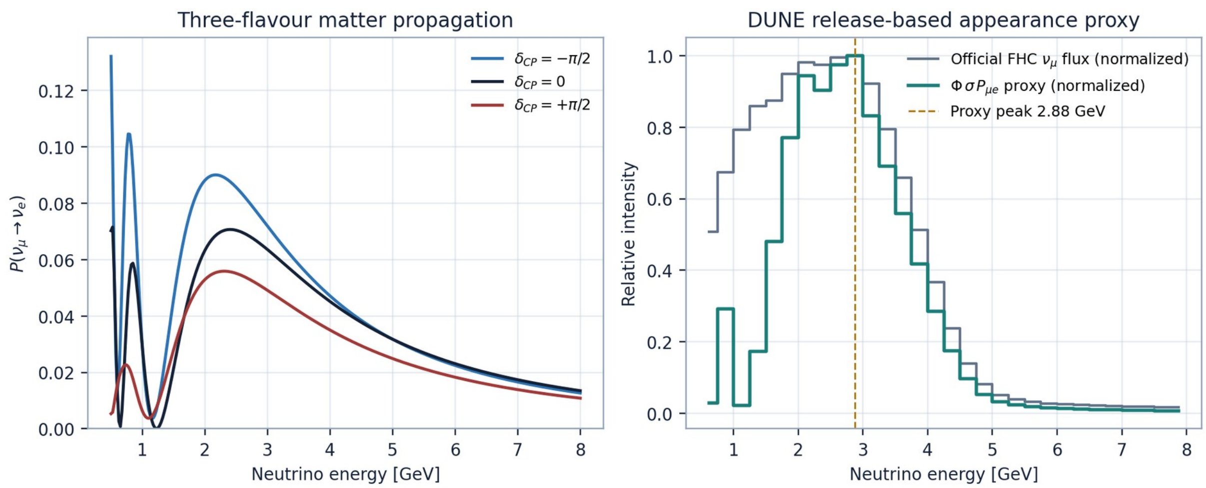

Figure 4. Standard three-flavour matter propagation and a DUNE release-based flux x cross-section x probability proxy.

DECISION

The standard Hamiltonian implementation passes the unitarity criterion by more than two orders of magnitude, and the release-based proxy is physically shaped. This validates the forecast code path. It says nothing about a nonzero H_ENDnu because that term was neither numerically specified nor fitted.

CROSS-EXPERIMENT SYNTHESIS

7. Combined validation decision

7.1 Evidence ledger

Program	Evidence	Validated object	Outcome	Inference ceiling
GWOSC	Observed public strain	Known inter-site delay and subband timing	Pass	Does not isolate END propagation
ATLAS	Observed educational collisions	Event reconstruction, likelihood, injection recovery	Pass	Not a publication-grade new-physics result
XENONnT	Observed events + released templates	Published WIMP benchmark limit	Pass in 5-12 GeV scope	No END particle point
DUNE	Released forecast configurations	Hamiltonian and flux-proxy calculation	Pass as forecast	No empirical DUNE data; H_ENDnu = 0

7.2 Final scientific statement

SUPPORTED

The observation-chain equations, event selection, detector-template use, profile-likelihood logic, injection/recovery mechanism, timing estimator, and standard oscillation propagator have been exercised on real or official public releases. All prespecified implementation-level criteria pass.

NOT SUPPORTED BY THESE TESTS

No unique END prediction has been confronted with the data. The analysis cannot choose or infer A_alpha, C/Lambda^2, an END dark-matter mass/cross section, or H_ENDnu without extending the theory beyond the supplied manuscript. Therefore END Theory is not empirically validated by this companion.

7.3 Falsifiable next step

The next edition should publish one immutable, machine-readable parameter card per claimed experiment. Each card must be timestamped and versioned before evaluation. At minimum it must contain the following fields.

Channel	Required frozen fields
GW	alpha; A_alpha with units/sign; propagation-distance integral; waveform phase correction; event set; prior
Collider	Operator basis; C_i/Lambda^2; cutoff and truncation rule; mediator mass/width if used; acceptance map; nuisance priors
Direct detection	m_chi; cross section or mediator parameters; halo model; nuclear response; detector template map
DUNE	Explicit Hermitian H_ENDnu(E,rho); flavour basis; sign conventions; nuisance priors; test statistic; release/config version

With these values fixed, the current code base can be extended from Level 1 standard-candle validation to Level 2 theory comparison: compute the END and null expectations, profile the same nuisance set, report goodness-of-fit and likelihood-ratio behavior, and perform coverage-calibrated pseudo-experiments. Until then, 'not established' is a methodological boundary, not a negative measurement of the framework.

REPRODUCIBILITY

Appendix A. Exact source hashes

The archive's SHA256SUMS.txt is normative for every packaged file. The hashes below are the primary inputs recorded in the machine-readable result ledger.

Program	File	SHA-256
GWOSC	H-H1_GWOSC_4KHZ_R1-1126259447-32.txt.gz	fefe8717306109460b6c9cff74da6beb9e80ee624824b4b09bdd2c54ce9b4dfc
GWOSC	L-L1_GWOSC_4KHZ_R1-1126259447-32.txt.gz	43d30a710d6ed4a8f27d13f45182f3825cbe99f87287b518618c8ff0e25e0d7c
CERN	data_A.4lep.root	bd50fbd4551ca446f5d53fd50a9749a81a899ea43d35c4899ebf887fb07ebe17
CERN	data_B.4lep.root	57e651a89f7911205d6163d3904e17b5df72e253559372128381ce041ac8b476
CERN	data_C.4lep.root	f0da7764a92d7f258596b621355a6d883610f46f605878ac992222fe846a39af
CERN	data_D.4lep.root	fa4f0f1ce7dd5ef7dfc9d1edcef82cc7da63418b124155842c7a84af909efc81
XENONNT	data/ac/template_XENONnT_sr0_ac_cevns.h5	981e2a4f1c962b7f94b3633ac81f95559536028ebc607324d55a2cd092ddb4e1
XENONNT	data/ac/template_XENONnT_sr1_ac_cevns.h5	9181399e04d0399d2b60dbfe5b6597cd5f494eefbd4587549d18265aba4deeae
XENONNT	data/b8/template_XENONnT_sr0_b8_cevns_tly_0.0_tqy_0.0.h5	93f6e1f455a9bbe6e7fe72d00e748f9101a21ed0fec68b01de576e62da260f1e
XENONNT	data/b8/template_XENONnT_sr1_b8_cevns_tly_0.0_tqy_0.0.h5	cbea05b5ce36b35a128445a601794cab86c98ecc91d53908cc8ddb21cc84fbb9
XENONNT	data/er/template_XENONnT_sr0_er_cevns.h5	8e3be75173f5ebeb0b79c153348ec5650e30a2721b99656a71164cdf6f70616c
XENONNT	data/er/template_XENONnT_sr1_er_cevns.h5	fdd561b774d9b661bf2ab2c5b969eaa339f3d08a92094d96206caf776bb89fda
XENONNT	data/rg/template_XENONnT_sr0_rg_cevns_tly_0.0_tqy_0.0.h5	a01ca8930f240d2feb75869093f84aa340bfc9aef320505ba072d2a32b98c538
XENONNT	data/rg/template_XENONnT_sr1_rg_cevns_tly_0.0_tqy_0.0.h5	02fe208f55a4ea82cb025e3551374bb9231c611b5d7f28c0ea22f65d04221cef
XENONNT	data/signal/wimp_si_spectrum_10.json	e439f5289e16e00eeb008f8b5a87aba67f58e971408f231570365515b6a45250
XENONNT	data/signal/wimp_si_spectrum_12.json	6aab419b0bf1a89546da4752f93f768f6e02fc553f8599bd8d96acdf63ac53df
XENONNT	data/signal/wimp_si_spectrum_3.json	d575840dec4a4f2b8c271c032e5dfa9897eba74ac62e8149a4e16f9977782be1
XENONNT	data/signal/wimp_si_spectrum_4.json	a529b6c5e464b4d6abf3cf1823da8289b493a478743a16e62a182e1e4be1eec7
XENONNT	data/signal/wimp_si_spectrum_5.json	d11b742c7bc97bdeaa8f0cbf0803d1474fa10967b62f12e154d231a8e88b3d20
XENONNT	data/signal/wimp_si_spectrum_6.json	dd9a654fdb69ee0c1f4ffd395c7afbc4408527793ac20718164f25de423713c4
XENONNT	data/signal/wimp_si_spectrum_8.json	9a4a3bcee95e10f134f99b3c2d97b7a6c124e50741a1d9cd43fca0632b633a81
XENONNT	data/wimp_si/template_XENONnT_sr0_wimp_si_10_cevns_tly_0.0_tqy_0.0.h5	812ff0509986b006504e1fc444ca12d18c9f485c588cab8c02c5d689fc0e4e85

Program	File	SHA-256
XENONNT	data/wimp_si/ template_XENONnT_sr0_wimp_si_12_cevns_tly_0.0_tqy_0.0.h5	491aa388d64e49536cf9fd351ef4f26d42c1cfaa95687c1e83c161d5374de62a
XENONNT	data/wimp_si/ template_XENONnT_sr0_wimp_si_3_cevns_tly_0.0_tqy_0.0.h5	8cf098c234b1f5d1e0fd4986ee267f28a295a4520fd09674b3fea74cbf747949
XENONNT	data/wimp_si/ template_XENONnT_sr0_wimp_si_4_cevns_tly_0.0_tqy_0.0.h5	cae02cbaff82de2119c5d485e3c4ab92dbddc0d21d485bfe197fb700dabf25c1
XENONNT	data/wimp_si/ template_XENONnT_sr0_wimp_si_5_cevns_tly_0.0_tqy_0.0.h5	e64be38114bcb25ca9c20345fb9265052b96b5967bd857a70a5cb4c23be5c830
XENONNT	data/wimp_si/ template_XENONnT_sr0_wimp_si_6_cevns_tly_0.0_tqy_0.0.h5	5e3b5a4de907501af82a1ca07503055dd297a3a0fa9b282c3d73f81d10d5c12c
XENONNT	data/wimp_si/ template_XENONnT_sr0_wimp_si_8_cevns_tly_0.0_tqy_0.0.h5	4c830dfa5c41027a2c403b9e995af4b568b2da1ecbeee6c411269eef241a99a7
XENONNT	data/wimp_si/ template_XENONnT_sr1_wimp_si_10_cevns_tly_0.0_tqy_0.0.h5	003640af12e6d987dff0a875719db3c212481e66be1abe92d9599a420cfb2049
XENONNT	data/wimp_si/ template_XENONnT_sr1_wimp_si_12_cevns_tly_0.0_tqy_0.0.h5	2cf95263656a19d025826558334d0aff41a614af11d335b58c944bf254a61e4a
XENONNT	data/wimp_si/ template_XENONnT_sr1_wimp_si_3_cevns_tly_0.0_tqy_0.0.h5	d1d9d65404e58b093fdab3dbec5f83f3689e23afa3ce707609564e09142cae02
XENONNT	data/wimp_si/ template_XENONnT_sr1_wimp_si_4_cevns_tly_0.0_tqy_0.0.h5	622627a81e9cc63a4f414d256f030a761263c6efa7199b70ff4ecd2ace6e6438
XENONNT	data/wimp_si/ template_XENONnT_sr1_wimp_si_5_cevns_tly_0.0_tqy_0.0.h5	a846c13be8a74c3f026f091a03a30f7a55de7c4d3129babba1c5faa5f3d6da6a
XENONNT	data/wimp_si/ template_XENONnT_sr1_wimp_si_6_cevns_tly_0.0_tqy_0.0.h5	d589e379f73ab5842b532fd5306da5701e482d51db16ed25965d7d0a0da734c9
XENONNT	data/wimp_si/ template_XENONnT_sr1_wimp_si_8_cevns_tly_0.0_tqy_0.0.h5	948d30ecb2053dbca0086286bb6141fefba4ea28eb184fbbe9b09222442dd817
XENONNT	limits/XENONnT_2024_SI.csv	096f5f8693ed8652c121656a07b812ae94cd9ae597e758475764660f9c536aff
XENONNT	real_data.pkl	5013f80b35819f84ddfc3d93b0e4e1ca80e35f25bd0d76b0a72ab028c35ceb44
DUNE	DUNE_GLoBES.glb	3ec19753e1e2e6bb6bb43b41a2f4cd01e7b85cc022550674a3d38fada0822aa9
DUNE	histos_g4lbne_v3r5p4_QGSP_BERT_OptimizedEngineeredNov2017_neutrino_LBNEFD_globes_flux.txt	0dd2eb8132eff8ea7d4bceaa1255a96bc95470262787d0b25e97ff8a21371500
DUNE	xsec_cc.dat	bb950e7fb645bc5cdb052d17e2076534be2cbfd24e83ddc851f6d906ece93efd

MACHINE-READABLE ARTIFACTS

Appendix B. Output inventory

Artifact	Purpose
validation_results.json	Primary result ledger, versions, checksums, scope, and final decision
gwosc_subband_timing.csv	Band definitions, lags, and injection quantiles
cern_selected_four_lepton_masses.csv	All 229 masses surviving the frozen selection
cern_four_lepton_histogram.csv	Observed and fitted values in the 105-160 GeV window
xenonnt_limit_reproduction.csv	Approximate and official limits, residuals, and scope flags
dune_oscillation_probabilities.csv	Neutrino and antineutrino appearance curves
dune_flux_appearance_proxy.csv	Flux, cross section, probability, and proxy values
figure_*.png	Four paper figures generated from the CSV/analysis state

Independent audit sequence

1. Verify the archive checksums before executing anything.
2. Create an isolated environment and install the pinned requirements.
3. Run the complete analysis with the frozen seed and included data subset.
4. Compare JSON and CSV values; inspect warnings or optimizer failures.
5. Review the scope flags before quoting any number as END-specific.
6. For changes, issue a new analysis version and retain the prior result ledger.

Numerical acceptance tolerances

Object	Acceptance
JSON/CSV deterministic rerun	Absolute 1e-10 or relative 1e-8 for floating values
GW timing	Exact sample-grid lag; published-interval decision unchanged
Optimizer results	Intervals and pass/fail decisions unchanged under platform-level float variation
Figures	Visual/data equivalence; byte identity not required

CRITICAL AUDIT

Appendix C. Limitations and robustness checks

Area	Limitation	Consequence
GWOSC source modelling	No inspiral waveform fit or cosmological distance kernel	Cannot infer A_alpha; timing-only result
GWOSC timing grid	Discrete cross-correlation at 4096 Hz	0.244 ms quantization; no sub-sample calibration
ATLAS selection	Uses first four stored leptons and a compact flavour/charge rule	Educational reconstruction, not collaboration event categorization
ATLAS background	Single exponential with no detector/systematic nuisance model	Local Z is diagnostic only
XENON statistics	Asymptotic threshold and nominal yields	Declared +/-30% scope; 3-4 GeV excluded
DUNE detector model	Appearance proxy stops before efficiency, migration, ND constraints, and nuisances	Shape/implementation forecast only
Theory closure	No experiment-specific END parameter card	No END-specific empirical likelihood

Robustness statements supported by this release

- All source inputs used by the executable are present and hashed.
- No random outcome is interpreted without a fixed seed and stated ensemble size.
- Pass/fail scopes are stored in the result ledger rather than inferred from the figures.
- Out-of-scope XENON threshold points are retained visibly, preventing selective omission.
- DUNE output is labelled forecast in code, JSON, figures, and prose.
- The final END decision follows from missing parameters, not from substituting Standard Model or WIMP benchmarks for END predictions.

PRIMARY SOURCES

References

[1] J. R. Evans, END Theory 2.0: The Evans Relational Framework - Technical Reference Edition, 8 August 2026.

[2] LIGO Scientific Collaboration and Virgo Collaboration, Observation of Gravitational Waves from a Binary Black Hole Merger, Physical Review Letters 116, 061102 (2016), DOI 10.1103/PhysRevLett.116.061102.

[3] Gravitational Wave Open Science Center, GW150914 event release and strain files, GW150914-v3.

[4] ATLAS Collaboration, ATLAS 13 TeV samples collection at least four leptons for 2020 Open Data release, CERN Open Data record 15005, DOI 10.7483/OPENDATA.ATLAS.2Y1T.TLGL.

[5] E. Aprile et al. (XENON Collaboration), First Search for Light Dark Matter in the Neutrino Fog with XENONnT, Physical Review Letters 134, 111802 (2025), DOI 10.1103/PhysRevLett.134.111802.

[6] XENON Collaboration, XENONnT Light WIMP data release, Zenodo DOI 10.5281/zenodo.14522706; source revision a09cd8fd77570dc2095f65f094fbcc114b634dfc.

[7] DUNE Collaboration, Experiment Simulation Configurations Approximating DUNE TDR, arXiv:2103.04797 (2021).

[8] DUNE Collaboration, Deep Underground Neutrino Experiment Far Detector Technical Design Report, Volume II: DUNE Physics, arXiv:2002.03005 (2020).

[9] G. Cowan, K. Cranmer, E. Gross, and O. Vitells, Asymptotic formulae for likelihood-based tests of new physics, European Physical Journal C 71, 1554 (2011), DOI 10.1140/epjc/s10052-011-1554-0.

[10] G. J. Feldman and R. D. Cousins, Unified approach to the classical statistical analysis of small signals, Physical Review D 57, 3873 (1998), DOI 10.1103/PhysRevD.57.3873.

Primary public links

- GWOSC GW150914
- CERN Open Data record 15005
- XENONnT public data
- XENONnT release repository
- DUNE TDR-approximation configurations
- DUNE public plot database

END OF VALIDATION COMPANION / ANALYSIS VERSION 1.0